Bamboo and Wood Structures

journal homepage: https://www.innoviair.cn/journal/BWS

Splitting Resistance of Timber Beams under Bolted Steel-Plate Connections Perpendicular to Grain: Experiments and Theoretical Analysis

Qili Zhou[a,*]

[a]*Yunnan University, Yunnan 650091, China*

ARTICLEINFO

Keywords:
Timber Structure
Bolted Connection
Perpendicular-to-Grain Loading
Splitting Capacity
Fracture Mechanics Parameter
Semi-Empirical Model

ABSTRACT

Timber structures offer advantages such as environmental sustainability and low carbon emissions. Among dowel-type connections, bolted connections with steel plates are widely used. However, the splitting capacity of timber beams under perpendicular-to-grain loading via such connections is influenced by multiple factors, leading to significant discrepancies among existing calculation formulas and results. Based on preliminary experimental research, this study tested a total of 113 timber beams and 6 bamboo glulam beams with steel plate bolted connections under perpendicular-to-grain loading. Specimens were categorized into two main groups based on member material type and total connection width. Results indicate that splitting capacity increases with the material density of wood and bamboo, exhibiting an essentially linear correlation. Furthermore, splitting capacity increases with total connection width until reaching a plateau beyond a certain width. Based on test results and current calculation models, a modified model for predicting the splitting capacity of bolted connections under perpendicular-to-grain loading is proposed. The average ratio of calculated to literature-reported experimental splitting capacities is 0.975. More importantly, this modified model considers a comprehensive set of influencing factors, offering broader applicability and improved usability for engineering design.

1.Introduction

Timber is a popular choice as a building material due to its sustainability, recyclability, waste efficiency, and low carbon footprint[1]. Both softwood and hardwood are utilized in modern timber structures, with growing research interest in hardwood, particularly regarding thermally modified engineered wood and the fire resistance of timber structures [2,3]. Steel plate bolted connections are among the most prevalent dowel-type connections. Perpendicular-to-grain loading is a common concern in such structures, necessitating design measures to mitigate its effects. Local tensile stresses perpendicular to the grain at connections can induce premature splitting and brittle failure, potentially resulting in a connection failure load significantly lower than the ductile bearing capacity predicted by models like the European yield model. Consequently, in such scenarios, the splitting capacity should exceed the design value derived from the European yield model. Design formulas for splitting capacity are addressed in Eurocode 5, CSA O86, and DIN 1024, while Chinese (GB 50005) and American (NDS) standards primarily specify minimum dimensional limits. Statistical analysis indicates that approximately 23% of 127 documented timber structure failures are attributable to connection failures, with dowel-type connections accounting for over half of these brittle failures[4]. Clearly, merely restricting bolt spacing, edge distance, and end distance is insufficient to ensure a ductile failure mode. Therefore, investigating the splitting behavior of

* Corresponding author.
E-mail addresses:zhouqili@163.com.
Received 07 September 2025; Received in revised form 18 October 2025; Accepted 10 November 2025; Available online 30 November 2025

timber structures under perpendicular-to-grain loading via steel plate bolted connections is of paramount importance.

Studies show that the splitting capacity of bolted connections is influenced by various factors, including timber member material type, cross-sectional dimensions, bolt configuration and quantity, loaded edge distance, and relative connection height. However, the precise relationships between some factors (especially member material and connection width) and splitting capacity require further clarification. To elucidate these relationships, this study conducted experiments on the splitting behavior of timber beams under perpendicular-to-grain loading by bolted connections, considering two primary variables: member material type and total connection width. Test results were compared with various models and design standards to assess their suitability. Furthermore, a revised calculation model for predicting the splitting capacity under such loading conditions is proposed. This refined model has been rigorously validated against experimental data from the literature, ensuring its accuracy and reliability.

2.Theoretical concepts

Major timber design codes provide various methods for calculating the splitting capacity under perpendicular-to-grain loading by steel plate bolted connections, but these methods are inconsistent, leading to significant variation in results. For instance, Eurocode 5[5] and CSA O86[6] adopt a calculation methodology based on linear elastic fracture mechanics (LEFM), pioneered by Van der Put[7]. Alternatively, based on the maximum tensile failure criterion, a semi-empirical calculation model was established[8], forming the theoretical basis for the formula in DIN 1052 – 2004[9]. In contrast, GB 50005[10] and NDS[11] primarily consider the yield bearing capacity based on the European yield model.

In LEFM-based models, the fracture mechanics parameter $k = (GG_c / 0.6)^{0.5}$ can be obtained by fitting experimental data, indirectly calculated from the fracture energy release rate G_c and shear modulus G, or directly tested via a simple tension test on single-dowel joints proposed by Yasumura[12]. However, values from the latter two methods show significant discrepancies, with the second method yielding excessively large values unsuitable for LEFM predictive frameworks[13]. In the maximum tensile failure criterion model, the definition of perpendicular-to-grain tensile strength involves factors like size effects, load duration, and moisture content[14]. Therefore, tensile strength values from small clear wood specimens cannot be directly applied.

The Van der Put model assumes the critical fracture energy release rate G_c is a mixture of modes I and II. Given only the relationship between G_{Ic} and G_{IIc} and the unknown mixing proportion, determining G_c precisely through experimentation is challenging. Therefore, G_c (indirectly represented by k is typically determined by fitting experimental data on splitting capacity. In Eurocode 5, for dowel-type connections, the maximum allowable design shear force $V_{max,d}$ on both sides of a connection is governed by the design splitting capacity $F_{90,d}$, for which a characteristic value $F_{90,k}$ is also provided. These equations enforce a shear force limitation, especially for multiple connections or a single connection positioned beyond the mid-span.

Based on modifications to the Van der Put model and test results, Ballerini[15] and Ballerini and Rizzi[16] proposed a semi-empirical model for calculating splitting capacity. This model, considering connection geometry, consists of three parts: $F_{90,1}$ (a revised Van der Put model for single-dowel connections), f_w (accounting for connection width), and f_c (accounting for connection height). However, the fitted fracture mechanics parameter k differs significantly from the Van der Put model, as it was derived from a best-fit analysis of average splitting capacities in Norway spruce beams with single-dowel connections.

Zarnani and Quenneville[17] proposed another semi-empirical model based on the Van der Put model for calculating splitting capacity across the entire beam cross-section under riveted connections. A key distinction in semi-empirical models is the use of the η factor, which captures the influence of unloaded end distance and connection net section width w_{net}. The Van der Put model assumes a point load at mid-span; thus, the η factor becomes crucial when the connection is near the beam end or load is distributed through multiple fastener rows. The Ballerini model also indicates that connection width influences splitting capacity, as ignoring this effect for multiple fastener rows is unrealistic.

Considering the Van der Put model, Leijten[18] proposed a revised version of the Eurocode 5 model. Incorporating a square root in the design model facilitates the straightforward introduction of a multiple connection reduction factor N. The revised model is expressed as splitting capacity rather than shear force. It also accounts for the detrimental effect of potential cracks via a crack factor k_{cr}, a nationally prescribed parameter in the Eurocode 5 National Annex. A parameter $k_G = 2k$ related to the fracture mechanics parameter is introduced. the relationship between the fracture mechanical parameter and wood density, where the square root of $(G_cG)$is equal to 0.048ρ-7.056, is cited from Schoenmaker[19], based on tests on three wood species (spruce, Iroko, Cumarú), albeit with only 5 data points per species.

Feng[20] studied factors affecting splitting capacity, such as distance between connections, connection height and width, connection position, and bolt number. It was confirmed that splitting capacity is about 1.4 times that of a single connection when the center distance between two connections exceeds twice the beam height. Combining advantages of the Van der Put and Ballerini models, a semi-empirical revised model was proposed.

3.Experimental test program

3.1.Materials and methods

Specimens were divided into two groups: one with varying member materials, the other with varying total connection width. Bolt spacing in both directions was four times the bolt diameter. Connections used 16 mm thick Q235 carbon steel side plates as loading devices and strength class 8.8 hexagon head bolts. Laboratory tests were designed to induce wood

splitting failures to maximize observations of the brittle failure mechanism.

The first group comprised 18 experimental series using six different simply supported beam materials: Chinese Xing'an larch glulam (G-L), Canadian Douglas fir glulam (G-DF), European spruce glulam (G-Y), LVL made from Northern Jiangsu fast-growing poplar (Y-LVL), LVL made from Northern Jiangsu whitebark pine (S-LVL), and bamboo glulam made from Hunan Phyllostachys pubescens (Z). Bamboo glulam served as a comparative material to assess model suitability for bamboo structures. Each series had three replicates. Steel plate bolted connections were positioned at mid-span with loaded edge distances of 75, 90, and 105 mm. Beam cross-sectional height was constant at 150 mm. Bolt patterns ($n_c \times n_r$) were 4×2, 4×3, and 2×2, with bolt diameters of 6 mm and 10 mm. Parameters are listed in Table 1, and specimen construction is shown in Fig 1.

The second group used Chinese Xing'an larch simply supported beams with symmetrically arranged mid-span connections (Fig 2). Bolt diameter was 10 mm, relative connection height α = 0.6. The total connection width, $2(l_r + s)$, increased from 0 to 440 mm in 40 mm increments (except 340 mm). When width exceeded 40 mm, connections were considered as two separate $n_c \times n_r = 2 \times 2$ connections, with spacing 2s (parallel to grain) varying from 0 to 360 mm in 40 mm increments (except 260 mm). Thirteen series were conducted, each with five replicates. Design parameters are in Table 2 (P-L: larch sawn timber; (2×2): assumed as two separate 2×2 connections). Intended beam height h was 150 mm; actual heights ranged 146–150 mm, mostly around 148 mm.

Table 1 Experimental details of the first group

Test Series	$l \times b \times h$ (mm×mm×mm)	h_e(mm)	$n_c \times n_r$	d (mm)	α
G-L1	1200×38×150	75	4×2	6	0.5
G-L2	1200×38×150	75	4×3	6	0.5
G-L3	1200×38×150	90	2×2	10	0.6
G-L4	1200×38×150	105	2×2	10	0.7
G-DF5	1200×38×150	75	4×2	6	0.5
G-DF6	1200×38×150	75	4×3	6	0.5
G-DF7	1200×38×150	90	2×2	10	0.6
G-DF8	1200×38×150	105	2×2	10	0.7
G-Y9	1200×38×150	75	4×2	6	0.5
G-Y10	1200×38×150	75	4×3	6	0.5
G-Y11	1200×38×150	90	2×2	10	0.6
G-Y12	1200×38×150	105	2×2	10	0.7
Y-LVL13	900×40×150	90	2×2	10	0.6
Y-LVL14	900×40×150	105	2×2	10	0.7
S-LVL15	900×40×150	90	2×2	10	0.6
S-LVL16	900×40×150	105	2×2	10	0.7
Z17	1200×38×150	90	2×2	10	0.6
Z18	1200×38×150	105	2×2	10	0.7

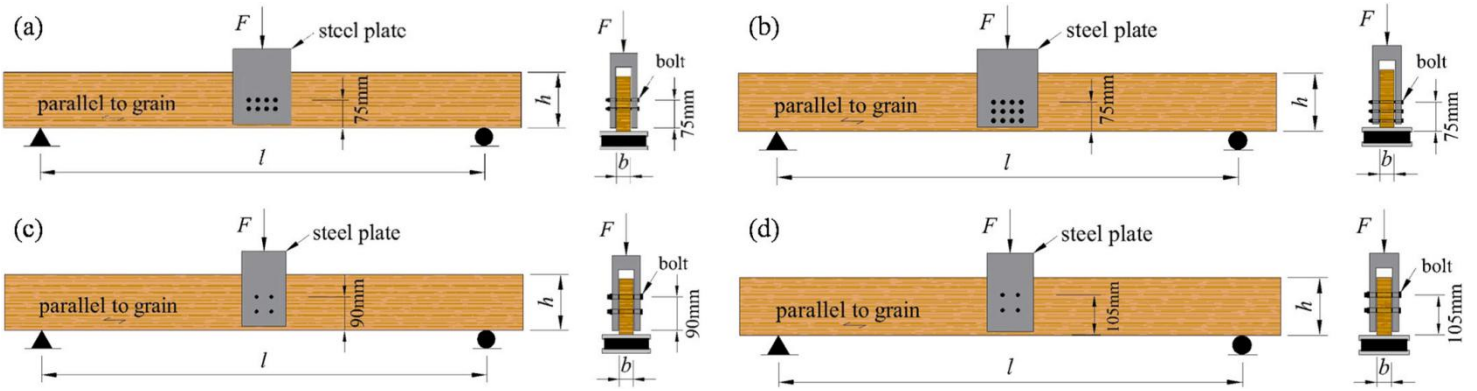

Fig 1. Construction diagram of the first group of specimens: (a) α=0.5, nc×nr=4×2, (b) α=0.5, nc×nr=4×3, (c) α=0.6, nc×nr=2×2 and (d) α=0.7, nc×nr=2×2.

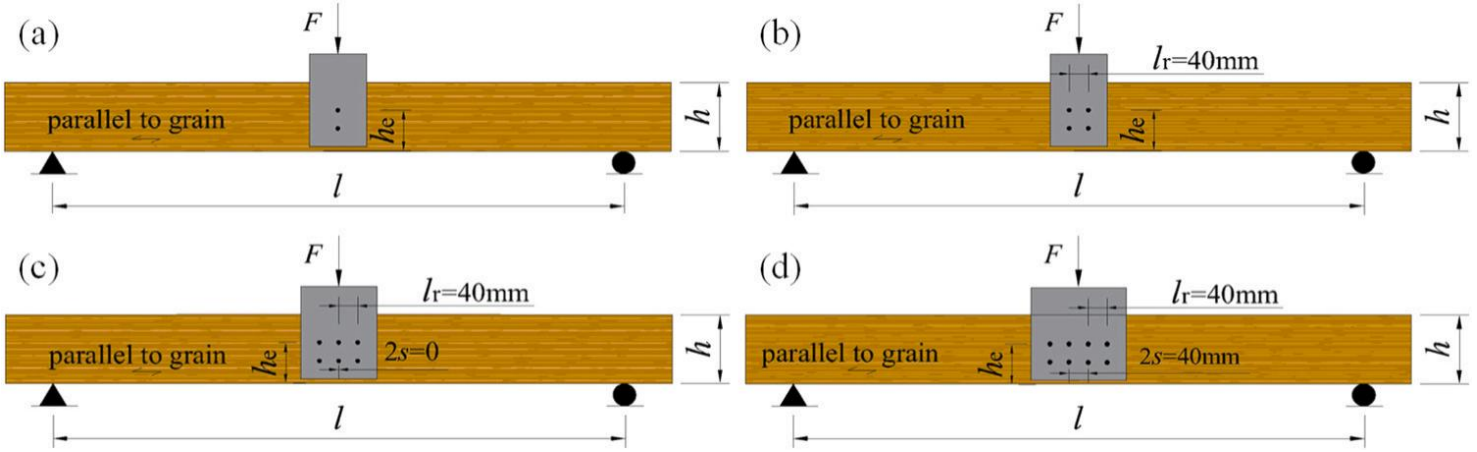

Fig 2. Construction diagram of the second group of specimens: (a) P-L1, (b) P-L2, (c) P-L3 and (d) P-L4.

Table 2 Experimental details of the first group

Test Series	$l \times b \times h$ (mm×mm×mm)	$n_c \times n_r$	$2s$ (mm)	l_r(mm)	l_1(mm)
P-L1	1100×38×148	1×2	0	0	0
P-L2	1100×38×148	2×2	0	40	0
P-L3	1100×38×148	3×2 (2×2)	0	40	40
P-L4	1100×38×148	4×2 (2×2)	40	40	80
P-L5	1100×38×148	4×2 (2×2)	80	40	120
P-L6	1100×38×148	4×2 (2×2)	120	40	160
P-L7	1100×38×148	4×2 (2×2)	160	40	200
P-L8	1100×38×148	4×2 (2×2)	200	40	240
P-L9	1100×38×148	4×2 (2×2)	240	40	280
P-L10	1100×38×148	4×2 (2×2)	260	40	300
P-L11	1100×38×148	4×2 (2×2)	280	40	320
P-L12	1100×38×148	4×2 (2×2)	320	40	360
P-L13	1100×38×148	4×2 (2×2)	360	40	400

3.2.Material properties

Air-dry density ρ_w, oven-dry density ρ_0, and moisture content W were measured per relevant Chinese standards: GB/T 1927.5 for sawn timber/glulam, GB/T 17657 for LVL, and GB/T 40487 for bamboo glulam. Thirty specimens were tested per material type; results are in Table 3.

To investigate the relationship between the fracture mechanics parameter k for different woods and splitting capacity, k was determined using Yasumura's single-bolt plate tensile test method. Specimen dimensions are shown in Fig 3, with 15 valid replicates per material. Tests used a CMT 5105 universal testing machine at 0.5 mm/min loading speed until splitting occurred at the bolt hole (duration ~5 – 10 min). Test setup is shown in Fig 4. The fracture mechanics parameter k was calculated using Eq. (1). Average failure load F and k values are in Table 4.

$$k = \frac{F}{2b\sqrt{h_e}} \quad (1)$$

Table 3 Physical properties of materials

Material	ρ_w (kg/m^3)	CV (%)	ρ_0 (kg/m^3)	CV (%)	W(%)	CV (%)
P-L	595	13.52	571	13.99	10.64	15.51
G-L	593	11.54	573	11.03	9.41	9.53
G-Y	478	4.23	450	4.23	10.29	7.79
G-DF	555	14.53	525	14.46	10.43	8.22
Y-LVL	618	3.10	598	3.13	8.91	11.81
S-LVL	665	4.97	638	5.00	10.23	6.40
Z	672	3.01	650	2.53	5.40	6.44

Table 4 Fracture mechanics parameters of single-bolt plate specimens.

Material	F (kN)	k (N.mm$^{-1.5}$)	CV (%)
P-L	7.19	15.10	15.13
G-L	7.41	15.41	8.30
G-Y	5.66	11.77	7.79
G-DF	6.88	14.32	8.22
Y-LVL	10.33	20.42	9.65
S-LVL	10.99	21.72	6.40
Z	9.67	20.11	15.74

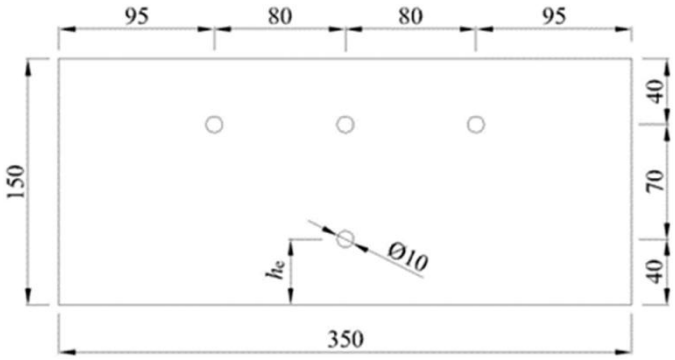

Fig 3. The design of specimen (unit: mm)

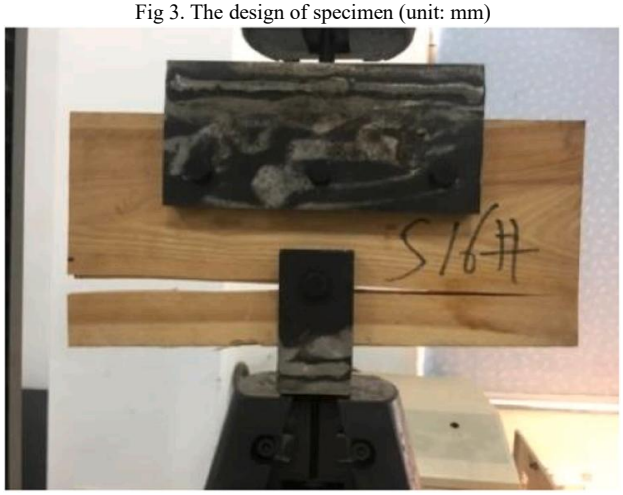

Fig 4. Test set-up

3.3.Test method

Load was applied via a hydraulic jack. Displacement measurement setup is shown in Fig 5. HVW model displacement transducers measured bolt slip. A BLR-1 type 100 kN tension-compression load sensor measured load. Data were recorded using a DH5922 dynamic strain testing system. Following ASTM D1761 (American Society of Testing Materials, 2012), displacement-controlled monotonic loading at 1.0-1.5 mm/min ensured failure within approximately 10 minutes.

4.Experimental observation and results

4.1.Failure mode

The brittle splitting failure process in simply supported beams with steel plate bolted connections typically followed three stages: 1) Audible fiber tearing sounds without visible cracks during initial loading; 2) More pronounced fracture sounds followed by minor short cracks forming at the bottom of bolt holes in the first row (farthest from beam bottom) as load increased; 3) Upon reaching critical load, cracks at the first-row bolt holes propagated rapidly towards both specimen ends with a loud noise, causing sudden brittle fracture.

Both specimen groups exhibited brittle splitting failure. The first group showed two main types: a crack along the grain cleanly splitting the beam, or a limited-length crack within the span, largely due to differences in pre-failure energy accumulation (Fig 6a, b). Pine LVL, poplar LVL, and

bamboo glulam beams often showed fiber bridging within cracks (Fig 6c), while larch, spruce, and Douglas fir members did not (Fig 6d). No noticeable compressive deformation around bolt holes or bolt deformation was observed (Fig 6e).

The second group exhibited splitting either at both connection positions (splitting beam into two halves) or confined to one connection (Fig 7).

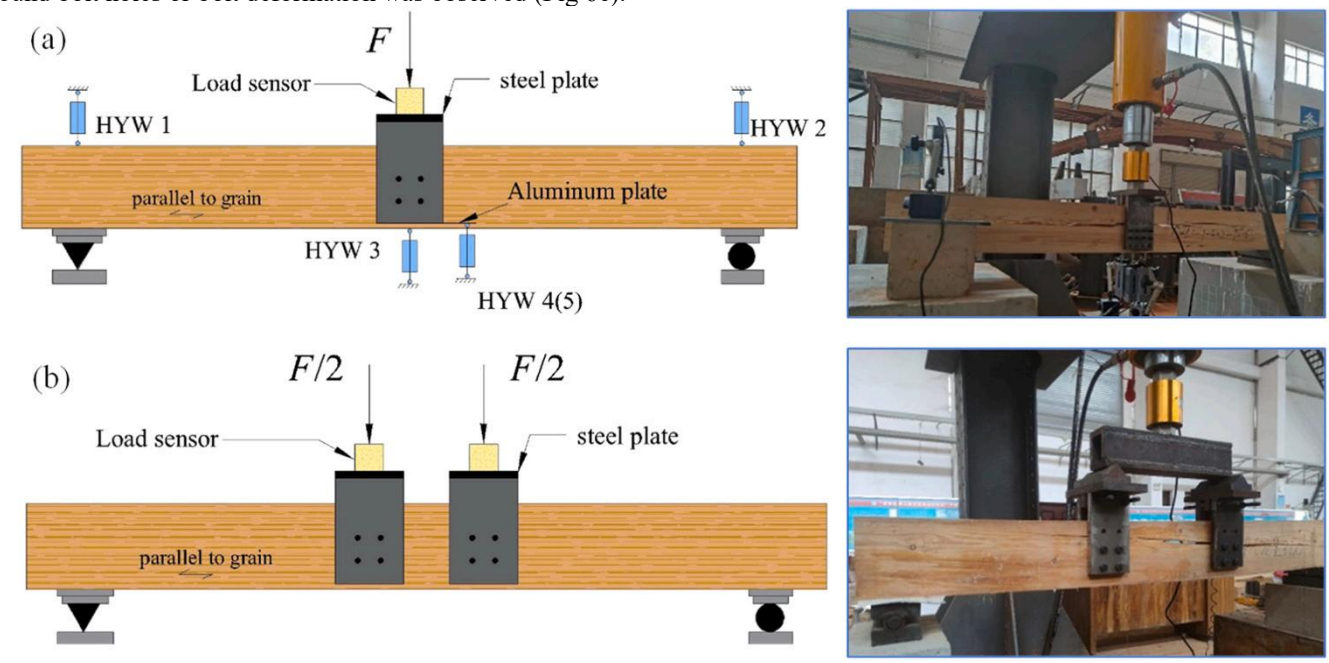

Fig 5. Test loading device: (a) the first group and (b) the second group

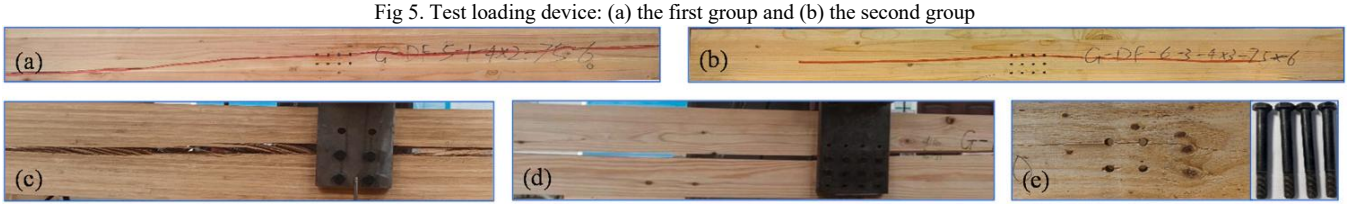

Fig 6. The splitting failure modes of the first group: (a) crack along the wood grain direction, (b) limited-length crack, (c) fiber bridging, (d) no fiber bridging and (e)undistorted bolt hole and bolt

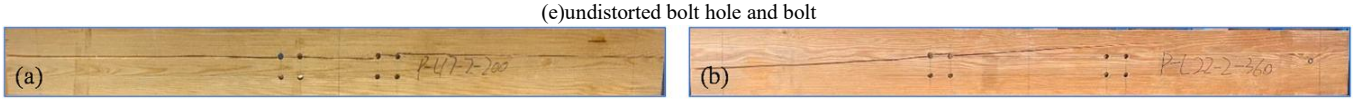

Fig 7. Test loading device: (a) the first group and (b) the second group

4.2.Load-slip curves

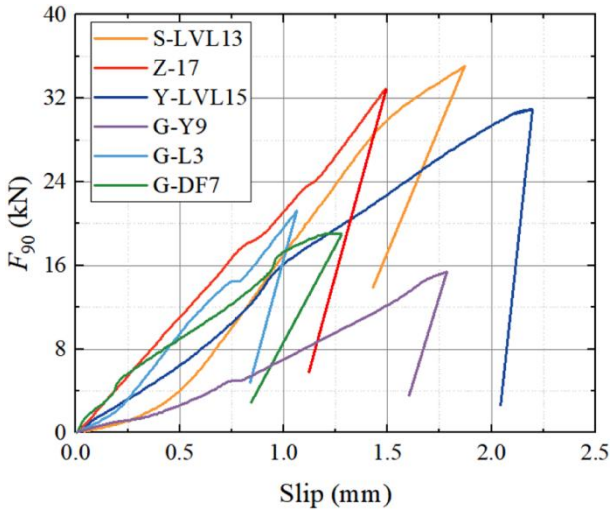

Fig 8. Typical load-slip curves of the first group

Fig 8 shows load-bolt slip curves for test series with $n_c \times n_r = 2 \times 2$ and $\alpha=0.6$. Linear elastic load-slip response up to failure is observed. When crack width at the connection reached ~1 mm, rapid crack propagation led to brittle splitting failure, consistent with experimental observations. Member material density significantly affected curve gradient and slip displacement: higher density generally resulted in a steeper slope. Failure slip displacement also relates to splitting capacity. Slight plastic compressive deformation at bolt holes occurred for poplar LVL, pine LVL, and spruce glulam, resulting in slip displacements exceeding 1.5 mm.

4.3.Splitting capacity

4.3.1.The first group

Fig 9 presents splitting capacity versus member material and bolt arrangement. To facilitate comparison across different beam widths (LVL: 45 mm, bamboo glulam: 60 mm, glulam: 80 mm), the ordinate shows splitting capacity per unit width (kN/mm) in Figs 9(c) and (d). Splitting capacity decreases with decreasing oven-dry density ρ_0. For identical bolt arrangements, splitting capacity shows an approximate linear correlation with ρ_0, particularly for glulam. Figs 9(a) and (b) show that splitting capacity increases with connection height h_e and number of bolts n_r . For example, increasing h_e from 40 mm to 80 mm and n_r from 8 to 12 increased splitting capacity by 0.94 kN to 3.22 kN, corresponding to a 4.16% – 20.96% increase, indicating significant impact. Figs 9(c) and

(d) show splitting capacity increases with relative connection height α. Increasing α from 0.6 to 0.7 increased splitting capacity by 0.53 – 6.41 kN, approximately 1.03 – 1.27 times.

Given the strong correlation between splitting capacity and density, density test blocks were taken near bolt holes of single-bolt plate specimens. The fracture mechanics parameter k was fitted against oven-dry and air-dry densities. A higher correlation was found with oven-dry density ρ_0 (Fig 10), expressed in Eq. (2):

$$k=0.05\rho_0-11.6 \quad (2)$$

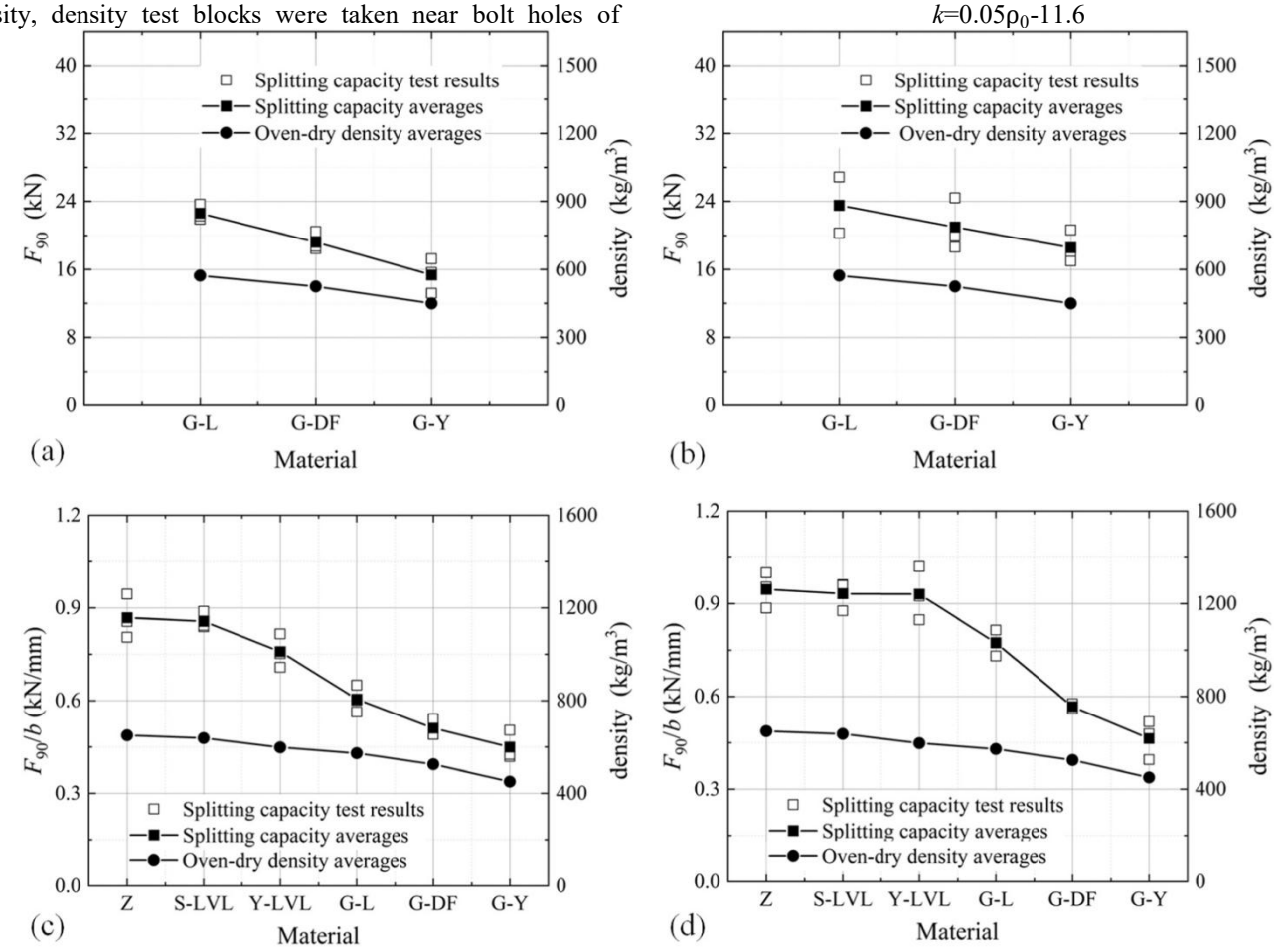

Fig 9. Relationship between material density and splitting capacity: (a) α=0.5, nc×nr=4×2, (b) α=0.5, nc×nr=4×3, (c) α=0.6, nc×nr=2×2 and (d) α=0.7, nc×nr=2×2

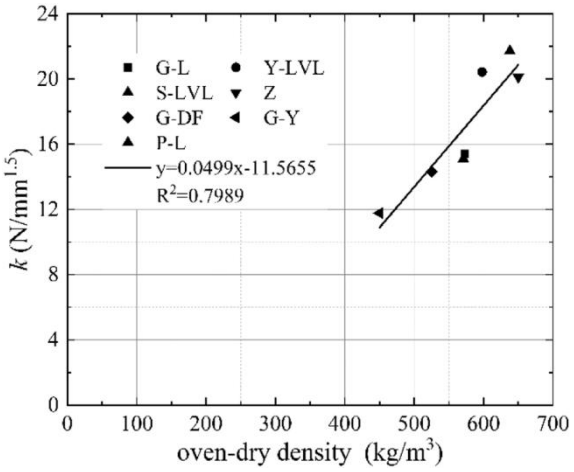

Fig 10. Relationship between the fracture mechanics parameter and the ovendry density

4.3.2.The second group

Fig 11 shows the relationship between total connection width $2(l_r + s)$ and splitting capacity. When $2(l_r + s)$ exceeds 200 mm (1.35h), splitting capacity plateaus. Below this threshold, capacity increases with width. When width exceeds 80 mm (treated as two separate 2 × 2 connections), splitting capacity gradually increases with center-to-center distance l_1 . When l_1 exceeds 160 mm, capacity ceases to increase significantly, stabilizing at 1.46 times that of a single connection. This observation contradicts the Ballerini, Ehlbeck, and DIN 1052-2004 models, which stipulate no interaction when $l_1 > 2h$, but shows similarity to the Leijten and Feng models, albeit with a different specific distance threshold.

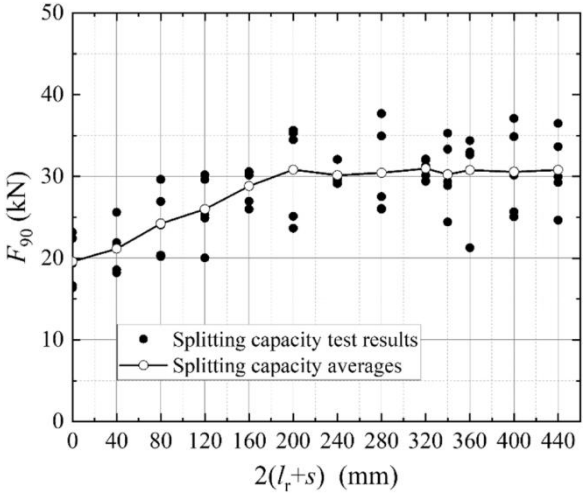

Fig 11. Impact of 2 (lr+s) on the splitting capacity

5.Discussion

5.1.Comparison of test results with existing models

Table 5 compares calculated and test values for five models: Eurocode 5, Ballerini, Zarnani, Leijten, and Feng. For Zarnani model on bamboo glulam, γ = 2.7. Series P-L5 to P-L13 are treated as two separate 2×2 connections.

Eurocode 5: Average ratio (calculated/test) = 0.64, CV = 24.93%. Significantly underestimates capacity with high variability due to using characteristic k values and not considering connection geometry or material differences.

Ballerini model: Average ratio = 0.78, CV = 23.30%. Shows significant variation for different materials with identical bolt arrangements. Conservative, especially for LVL and bamboo glulam, because k was derived solely from European spruce. Underestimates capacity in the second group; stabilization occurs at 1.35h vs. model's 1.6h prediction.

Feng model: Average ratio = 0.97, CV = 7.07%. Shows excellent agreement (0.99 for first group). Uses measured k values from Table 4.

Zarnani model: Average ratio = 0.77, relatively conservative. Also uses measured k values, indicating inadequate consideration of connection geometric parameters.

Leijten model: Average ratio = 1.35, overestimates capacity, suggesting its formula for k requires optimization.

For the second group, the Feng model shows close correlation but slight conservatism. The Zarnani model is more conservative, especially when treating connections as separate. Its calculated/test ratio increases with spacing until $l_1 = 2h$, indicating its interaction assumptions are more appropriate beyond that spacing. The Leijten model overestimates capacity, especially when $l_1 < 2h$ or when treating as separate connections with $l_1 > 2h$, highlighting deficiencies in its k calculation.

Overall, the Feng model aligns best with test data. However, it requires measuring k via single-bolt plate tests, which is impractical for designers. Moreover, within a specific total width range, it conservatively uses center spacing as the dominant variable, neglecting the detrimental effects of connection width l_r, leading to inaccuracies and discontinuity in the width parameter f_w when l_1 is between 1.35h and 1.62h, necessitating refinement.

Table 5 Comparisons of model calculated values with test values.

Test Series	Test result	CV (%)	Calculated value/Test value				
			Eurocode 5	Ballerini model	Zarnai model	Leijten model	Feng model
G-L1	22.60	4.08	0.58	0.79	0.78	1.20	0.90
G-L2	23.54	14.02	0.55	0.90	0.75	1.16	1.01
G-L3	22.97	7.14	0.69	0.67	0.81	1.45	0.93
G-L4	29.38	5.43	0.68	0.62	0.78	1.41	0.91
G-DF5	19.20	5.64	0.68	0.93	0.86	1.30	0.99
G-DF6	20.98	14.48	0.62	1.01	0.78	1.19	1.05
G-DF7	19.41	5.23	0.82	0.80	0.89	1.57	1.02
G-DF8	21.55	1.45	0.94	0.85	0.99	1.77	1.15
G-Y9	15.36	13.31	0.85	1.16	0.88	1.32	1.02
G-Y10	18.58	10.07	0.70	1.14	0.73	1.09	0.98
G-Y11	17.08	10.57	0.93	0.90	0.83	1.46	0.96
G-Y12	17.62	13.53	1.13	1.03	1.00	1.76	1.16
LVL-Y13	30.33	7.18	0.55	0.54	0.84	1.22	0.98
LVL-Y14	37.23	9.27	0.56	0.52	0.85	1.24	1.00
LVL-S15	34.27	3.22	0.49	0.47	0.79	1.19	0.93
LVL-S16	37.29	5.20	0.56	0.51	0.90	1.36	1.06
Z17	33.00	8.13	0.48	0.47	0.73	1.19	0.85
Z18	35.97	6.08	0.55	0.51	0.83	1.36	0.97
Mean			0.69	0.77	0.83	1.35	0.99
CV (%)			26.19	30.70	9.30	14.56	8.03
P-L1	19.59	16.09	0.81	0.65	0.87	1.69	0.97
P-L2	21.14	14.13	0.75	0.73	0.85	1.57	0.98
P-L3	24.23	16.98	0.65	0.74	0.79	1.37	0.93
P-L4	25.99	15.85	0.61	0.79	0.79	1.28	0.94
P-L5	28.81	7.55	0.55	0.80	0.53	1.15	0.91
P-L6	30.83	19.25	0.51	0.83	0.53	1.08	0.87
P-L7	30.13	3.80	0.52	0.85	0.57	1.10	0.89
P-L8	30.44	18.00	0.52	0.84	0.60	1.09	0.96
P-L9	30.97	3.81	0.51	0.82	0.62	1.07	0.95
P-L10	30.23	13.98	0.52	0.84	0.65	1.55	0.97
P-L11	30.77	17.47	0.51	0.83	0.66	1.52	0.95
P-L12	30.55	17.61	0.52	0.83	0.70	1.53	0.96
P-L13	30.78	14.66	0.51	0.83	0.72	1.52	0.95
Mean			0.58	0.80	0.68	1.35	0.94
CV (%)			17.52	7.30	16.88	16.88	3.48

5.2.Modification of existing models

To improve accuracy and applicability, the Feng model is modified based on test results, focusing on member material and connection width influences. The modified model is detailed in Eqs. (3)-(6). The expression for k is updated to Eq. (4) based on single-bolt tensile tests. The connection width parameter f_w is updated to Eq. (5) based on the second group tests, derived from the fitting curve in Fig 12 (vertical axis: ratio of each group's average test value to the mean of series P-L1 and P-L2).

When treating the steel plate bolt connection as a single entity, its total width $2(l_r + s)$ has a limited impact, not exceeding 1.55 times the capacity of a single-column connection. When viewed as two separate connections, capacity plateaus when total width reaches 1.35h (where 2s = 0.81h), approximating 1.46 times a single connection's capacity, aligning with Leijten and Feng model conclusions. In the revised model, f_w incorporates both l_r and 2s, with 2s as the dominant factor, mitigating issues from overly wide connections/narrow spacings and ensuring continuity when 2s = 0.81h.

$$F_{90} = 2f_w f_c bk\sqrt{\frac{h_e}{1-\alpha}} \tag{3}$$

$$k=0.05\rho_0-11.6 \tag{4}$$

$$f_w=\begin{cases}1+0.41\frac{2(l_r+s)}{h}\le 1.55 & N=1\\ \left(1+0.41\frac{l_r}{h}\right)1.46 & N=2, l_r\neq 0 \text{ and } 2s=0.81h\end{cases} \tag{5}$$

$$f_c = 1 + 1.52\frac{n_r h_c}{1000+n_r h_c} \tag{6}$$

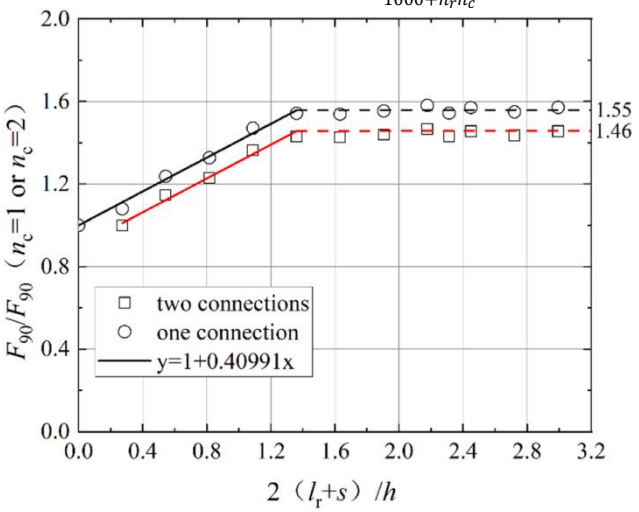

Fig 12. The fitting results the connection width parameter f_w

5.3.Verification of the modified model

Verification of k formula: The formula for k (Eq. 4) was assessed using test data from 333 single-bolt/dowel connections in literature (Jensen et al., 2015; Ballerini, 2004; Feng, 2020; Reshke, 1999; Ballerini, 2003; Finkenbinder, 2007; Patel, 2009; Wang, 2018; Feng et al., 2021; Majano-Majano et al., 2022; Gomez-Royuela et al., 2024). Material densities (air-dry converted to oven-dry per ASTM D2395) are in Table 6. Fig 17 compares calculated vs. literature test values. The ratio ranges 0.69 – 1.22, averaging 0.932 with CV = 17.8%. Although slightly conservative, the proposed k formula is reasonably applicable, even for bamboo glulam.

Verification of f_w formula: The connection width parameter f_w was verified against 557 datasets from literature (same sources as above plus Ballerini, 1999; Kasim, 2002; Kasim & Quenneville, 2003), including New Zealand Radiata pine, Iroko, and Brazilian Cumarú. Connections were at mid-span with total width-to-height ratio from 0 to 4.7. Calculated values from Ballerini, Zarnani, Feng, and the modified model were compared to test values (Figs. 15 – 18). In Feng and Zarnani models for this comparison, k was obtained using the same method as the modified model (Eq. 4).

Ballerini model (Fig 13): Avg. ratio = 0.82 (range 0.48 – 1.21), CV = 32.26%. Poor applicability due to fixed k=14 and unstable ratio with varying connection width.

Zarnani model (Fig 14): Avg. ratio = 0.79 (range 0.50 – 1.16), CV = 24.08%. Conservative with less dispersion than Ballerini but decreased stability for large fastener spacings, indicating need to refine width treatment.

Feng model (Fig 15): Avg. ratio = 0.951 (range 0.65 – 1.32), CV = 21.54%. Good fit but exhibits discontinuity in f_w as previously noted.

Modified model (Fig 16): Avg. ratio = 0.975 (range 0.68 – 1.31), CV = 21.44%. Best agreement with literature. Ratio remains essentially unchanged with increasing connection width. Compared to Feng model, when l_r = 0, the difference in ratios widens as center spacing l_1 increases (max diff. ~10%), because Feng model peaks when l_1 > 1.17h, while modified model peaks when l_1 > 1.35h. More importantly, the modified model avoids adverse effects from unconstrained net width changes and ensures f_w continuity, offering a more comprehensive consideration of connection width impact.

When the total width/height ratio exceeds 1.0, the modified model's average ratio to literature values is 0.869 (slight underprediction), primarily because the member material in those cases is spruce-pine. For single-bolt spruce-pine connections (Fig 17), the average ratio is 0.821.

Table 6 Density of member materials in the literatures.

material	Specimen Quantity	ρ_w (kg/ m^3)	W (%)	ρ_0 (kg/ m^3)
southern pine LVL	22	-	-	640
The southern pine glulam	34	-	-	560
Yellow-poplar PSL	29	-	-	630
Spanish Eucalyptus globulus	24	808	12	782
Xing'an Larch	9	-	-	591
The US yellow poplar LVL	45	-	-	580
The US southern pine LVL	22	-	-	655
European spruce	78	430	10	405
New Zealand Douglas fir	9	516	12.5	484
Spruce-pine	30	450	11	422
bamboo glulam	9	-	-	592
European beech	22	732	12	703

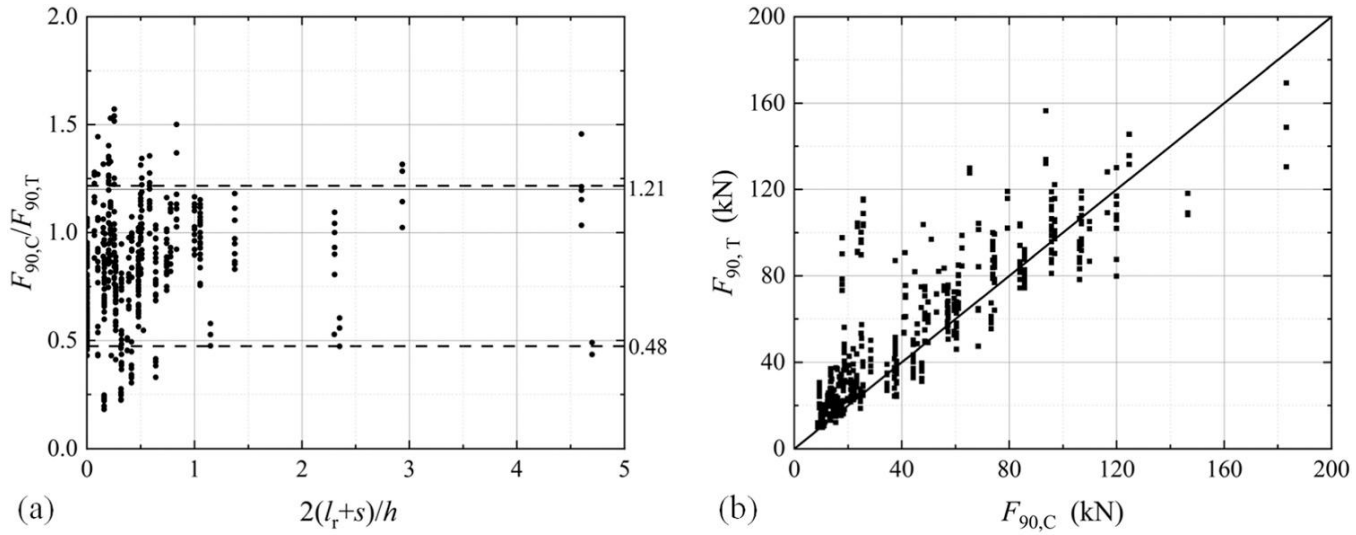

Fig 13. Comparison Results of Ballerini Model: (a) the impact of fw and (b) calculated value to test value

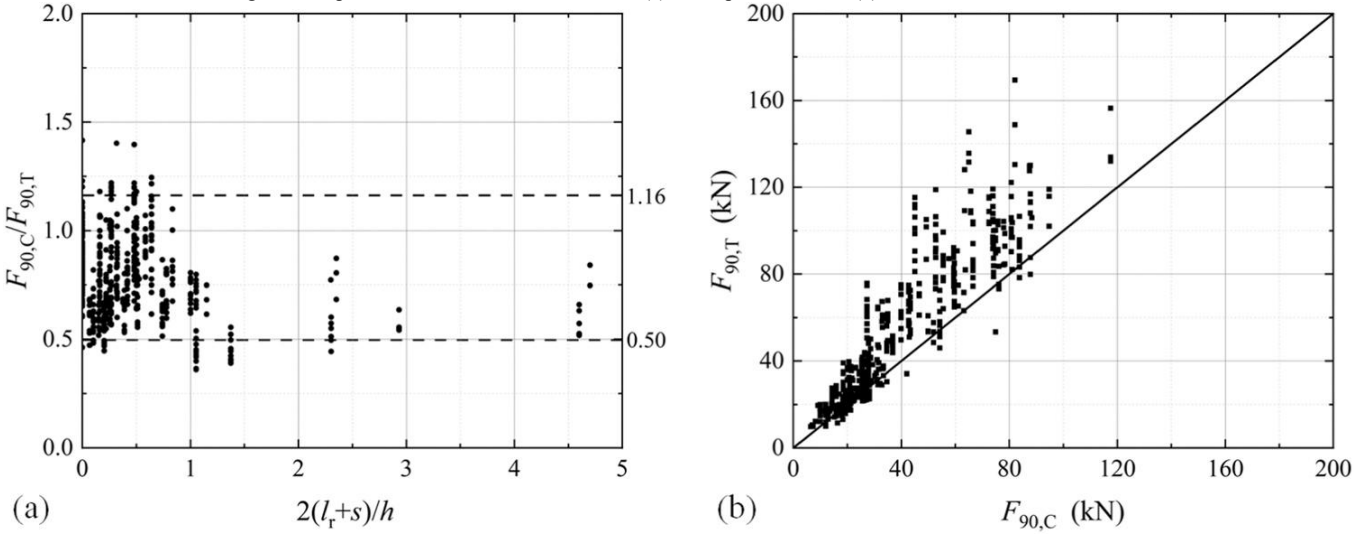

Fig 14. Comparison Results of Zarnani Model: (a) the impact of fw and (b) calculated value to test value

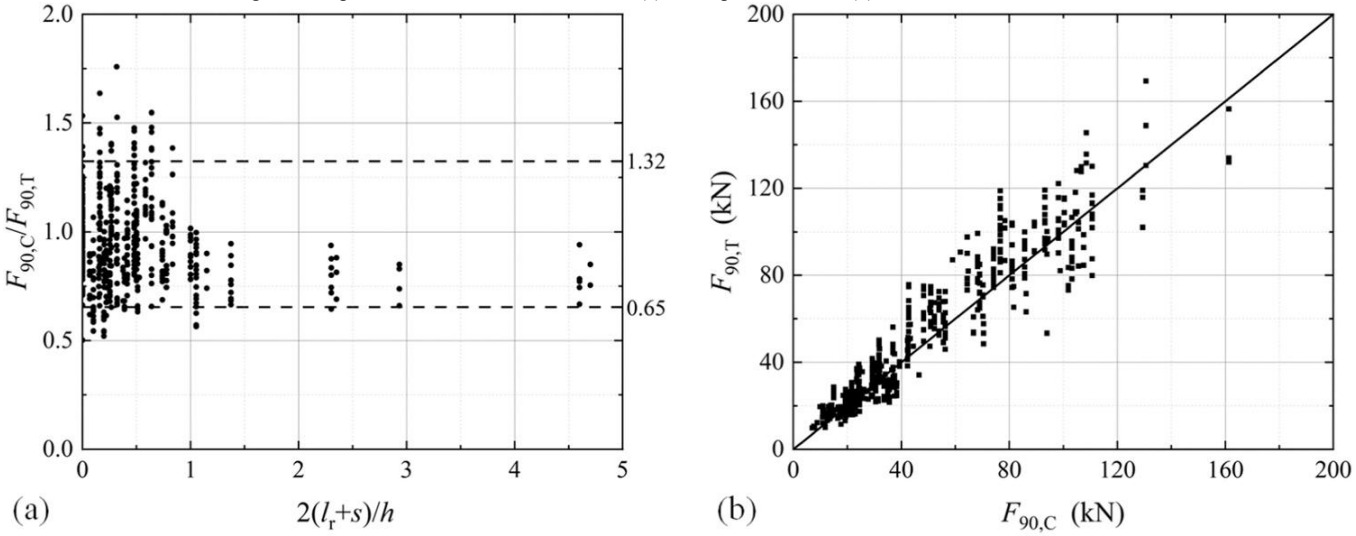

Fig 15. Comparison Results of Feng model: (a) the impact of fw and (b) calculated value to test value

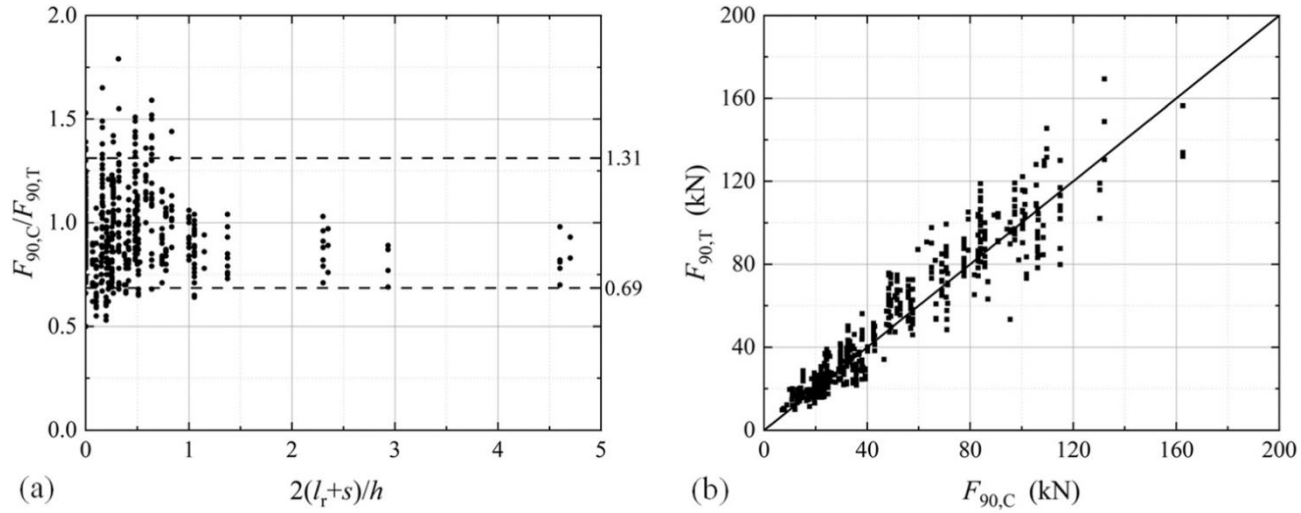

Fig 16. Comparison Results of Modified model: (a) the impact of f_w and (b) calculated value to test value

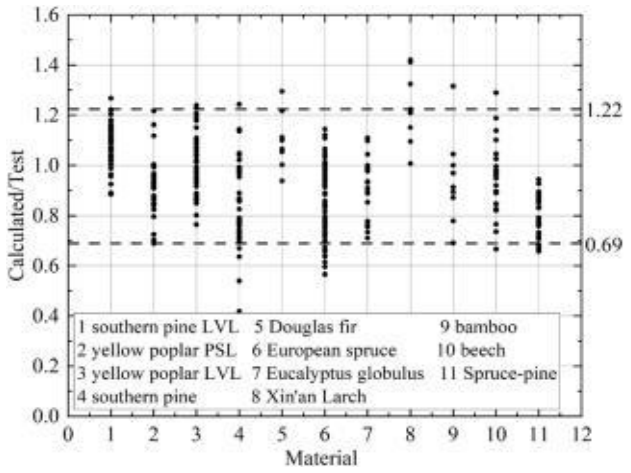

Fig 17. Ratios of calculated value to test value versus member-density

6.Conclusions

Experimental and theoretical research investigated the splitting capacity of timber beams with steel plate bolted connections under perpendicular-to-grain loading, focusing on member materials and connection width. A modified calculation model is proposed. Key findings:

(1) Splitting capacity varies significantly among member materials, primarily due to density differences. An empirical formula relating the fracture mechanics parameter to oven-dry density was established from single-bolt plate tensile tests, directly linking splitting capacity calculation to member material density.

(2) Splitting capacity increases with total connection width until reaching a plateau at 1.35 times the beam height, where it is 1.55 times that of a single-column connection. When treated as two separate connections, total capacity peaks at 1.46 times a single connection's capacity when the spacing between them reaches 0.81h.

(3) A semi-empirical modified model is proposed. For single-bolt connections across various materials, the model shows an average calculated-to-literature ratio of 0.932 (CV=17.8%), demonstrating reasonable applicability, albeit slightly conservative, including for bamboo glulam. For multi-bolt connections, the average ratio is 0.975. The model better considers member materials and connection geometry, offering wider applicability and more convenient use for engineering design.

References

[1] TANTHANAWIWAT K, GHEEWALA S H, NILSALAB P, et al. Environmental Sustainability and Cost Performances of Construction and Demolition Waste Management Scenarios: A Case Study of Timber and Concrete Houses in Thailand. Journal of Cleaner Production, 2024, 436: 140652.

[2] YUE K, QIAN J, WU P, et al. Experimental Analysis of Thermally-Treated Chinese Poplar Wood with Focus on Structural Application. Industrial Crops and Products, 2023, 197: 116612.

[3] LI X, YUE K, ZHU L, et al. Relationships Between Wood Properties and Fire Performance of Glulam Columns Made from Six Wood Species Commonly Used in China. Case Studies in Thermal Engineering, 2024, 54: 104029.

[4] HANSSON E F. Analysis of Structural Failures in Timber Structures: Typical Causes for Failure and Failure Modes. Engineering Structures, 2011, 33: 2978–2982.

[5] EUROPEAN COMMITTEE FOR STANDARDIZATION. *Eurocode 5: Design of Timber Structures – Part 1-1: General – Common Rules and Rules for Buildings: EN 1995-1-1. Brussels, Belgium: European Committee for Standardization, 2004.

[6] CANADIAN STANDARDS ASSOCIATION. *Engineering Design in Wood: CSA 086-2019. Mississauga, Canada: Canadian Standards Association Group, 2019.

[7] VAN DER PUT T A C M. Tension Perpendicular to the Grain at Notches and Joints//Proceedings of the 23th International Council for Research and Innovation in Building and Construction, CIB-W18 Meeting. Karlsruhe, Germany: International Council for Research and Innovation in Building and Construction, 1990.

[8] EHLBECK J, GORLACHER R, WERNER H. Determination of Perpendicular-to-Grain Tensile Stresses in Joints with Dowel-Type Fasteners - A Draft Proposal for Design Rules//Proceedings of the 22th International Council for Research and Innovation in Building and Construction, CIB-W18 Meeting. Karlsruhe, Germany: International Council for Research and Innovation in Building and Construction, 1989.

[9] GERMAN INSTITUTE FOR STANDARDIZATION. *Design of Timber Structures: General Rules and Rules for Buildings: DIN 1052-2004. Berlin, Germany: German Institute for Standardization, 2008.

[10] NATIONAL STANDARDS OF THE PEOPLE’S REPUBLIC OF CHINA. *Standard for Design of Timber Structures: GB 50005-2017. Beijing: China Architecture & Building Press, 2017.

[11] AMERICAN NATIONAL STANDARDS INSTITUTE. *National Design Specification for Wood Construction: NDS-2024. Washington, DC, USA: American Wood Council, 2024.
[12] YASUMURA M. Determination of Fracture Parameter for Dowel-Type Joints Loaded Perpendicular to Timber Grain and Its Application//Proceedings of the 35th International Council for Research and Innovation in Building and Construction, CIB-W18 Meeting. Karlsruhe, Germany: International Council for Research and Innovation in Building and Construction, 2002.
[13] JENSEN J L, QUENNEVILLE P, GIRHAMMAR U A, et al. Brittle Failures in Timber Beams Loaded Perpendicular to Grain by Connections. Journal of Materials in Civil Engineering, 2015, 27(11): 04015026.
[14] JOCKWER R, DIETSCH P. Review of Design Approaches and Test Results on Brittle Failure Modes of Connections Loaded at an Angle to the Grain. Engineering Structures, 2018, 171: 362–372.
[15] BALLERINI M. A New Prediction Formula for the Splitting Strength of Beams Loaded by Dowel Type Connections//Proceedings of the 37th International Council for Research and Innovation in Building and Construction, CIB-W18 Meeting. Karlsruhe, Germany: International Council for Research and Innovation in Building and Construction, 2004.
[16] BALLERINI M, RIZZI M. Numerical Analyses for the Prediction of the Splitting Strength of Beams Loaded Perpendicular-to-Grain by Dowel-Type Connections. Materials and Structures, 2007, 40(1): 139–149.
[17] ZARNANI P, QUENNEVILLE P. Splitting Strength of Small Dowel-Type Timber Connections: Rivet Joint Loaded Perpendicular to Grain. Journal of Structural Engineering, 2014, 140(10): 04014064.
[18] LEIJTEN A J M. Splitting of Timber Beams Caused by Perpendicular to Grain Forces of Multiple Connections. Engineering Structures, 2018, 171: 10–14.
[19] SCHOENMAKER J C M. Fracture and Failure Mechanisms in Timber Loaded Perpendicular to the Grain by Mechanical Connections. Eindhoven, the Netherlands: Eindhoven University of Technology, 2010.
[20] FENG X. Research on Mechanical Performances of Timber Members Loaded Perpendicular to Grain by Bolted Connections. Changsha, China: Central South University of Forestry and Technology, 2020.